Scientific Research Publishing

World Journal of Nuclear Science and Technology, 2025, 15(3), 111-134
https://www.scirp.org/journal/wjnst
ISSN Online: 2161-6809
ISSN Print: 2161-6795

A Case Study of the Susceptibility of Zircaloy-4 Sheathing to Iodine Stress-Corrosion Cracking as a Function of Their Metallurgical History in Fabrication

Mohsen Farahani[1*], Paul K. Chan[2], Jennifer L. Snelgrove[3], Diane Wowk[4]

[1]Department of Chemical Engineering, Queen's University, Kingston, Canada
[2]Clean Core Thorium Energy, Inc., Chicago, IL, USA
[3]Department of Chemistry and Chemical Engineering, Royal Military College of Canada, Kingston, Canada
[4]Department of Mechanical and Aerospace Engineering, Royal Military College of Canada, Kingston, Canada
Email: *Farahani@kommyF.org

How to cite this paper: Farahani, M., Chan, P.K., Snelgrove, J.L. and Wowk, D. (2025) A Case Study of the Susceptibility of Zircaloy-4 Sheathing to Iodine Stress-Corrosion Cracking as a Function of Their Metallurgical History in Fabrication. *World Journal of Nuclear Science and Technology*, **15**, 111-134.
https://doi.org/10.4236/wjnst.2025.153009

Received: June 23, 2025
Accepted: July 22, 2025
Published: July 25, 2025

Abstract

This experimental undertaking has primarily focused on determining the dependency of Pellet-Cladding Mechanical Interaction (PCMI) conditions and the resulting Iodine Stress-Corrosion Cracking (ISCC) failures on residual stresses within a wide range of manufactured CANDU Zircaloy-4 cladding (sheathing). ISCC failures remain a fuel performance concern for water-cooled reactors, including CANDU reactors, accommodating a multitude of power maneuverability events, at high discharge burnups. A multi-year examination of more recent and vintage Zircaloy-4 sheathing samples and their associated post-production stress state from two independent sources is provided. A relationship between the residual stress history in manufacturing processes of Zircaloy-4 and ISCC has been investigated, by static loading of slotted ring samples in iodine-methanol solutions (10 $g \cdot L^{-1}$) at room temperature. Results indicate that inherent residual tensile stress state of the sheathing above a certain threshold is strongly correlated to the failure in ISCC process.

Keywords

CANDU Zircaloy-4 Fuel Cladding (Sheathing), Post-Production Residual Stress History, Pellet-Cladding Mechanical Interaction, Iodine Stress-Corrosion Cracking

1. Introduction

Pellet-Cladding Mechanical Interaction and Iodine-Induced Stress-Corrosion Cracking

Zirconium and its alloys (>98% Zr) have hexagonal close packed (hcp) crystal structure and exhibit highly reproducible anisotropic thermal, elastic and plastic properties, due to thermo-mechanical processing route adopted by the industry to fabricate a tube product that meets or exceeds service requirements. Much of the latter credit is due to metal producers and fabricators for their operational culture. Zircaloy-4 (UNS R60804), in particular, is the backbone in-core structural materials in thermal reactors such as CANDU reactors, by virtue of a superior combination of intrinsic properties, such as compatibility with uranium oxide, low neutron absorption cross section, high melting point, good thermal conductivity, low thermal expansion and high temperature creep behavior, Stress-Corrosion Cracking (SCC) resistance, reduced hydrogen uptake and its resulting embrittlement, and oxidation stability.

Pellet-Cladding (sheathing) Mechanical Interactions (PCMI) have been recognized as the cornerstone of major fuel sheathing reliability shortcomings in the form of sheathing service failures since 1970s, at times proving insidious and costly [1]. PCMI origin dates back to the testing of General Electric Vallecitos Boiling Water Reactor using enriched uranium and stainless-steel sheathing material in 1963, and subsequent elucidation that Iodine Stress-Corrosion Cracking (ISCC) was the underlying cause, was published in 1965 [2]. The onset of systemic failures reached a high point, when on-line refuelling in the CANDU-prototype Nuclear Power Demonstration (NPD) reactors and Douglas Point had started in 1969, with further escalation with the start-up of Pickering-1 (the first CANDU full-scale plant) in 1971 [3]. The PCMI has its roots in simultaneous evolution of local chemical and mechanical stresses inside Zircaloy sheathing, physically encapsulating the uranium dioxide fuel (UO_2) pellets, and acting as first full retention barrier between the radioactive fuel and exterior coolants [4]. Under mechanical stress, UO_2 pellet expansion induces a strain-controlled loading on the sheathing at approximately 1 s^{-1} circumferential strain rate [5]. This phase is referred to as PCMI (Pellet Cladding Mechanical Interaction).

The following synergy of environmentally assisted requirements for the initiation of ISCC in the Zircaloy sheathing have been identified [6]: i) a critical increase in local stress, or strain from UO_2 pellet expansion; ii) a corrosive environment provided by volatile fission products, predominately iodine; iii) a minimum incubation time; and iv) a susceptible material. The spectrum of combined concentration of factors on the ISCC susceptibility of Zircaloy sheathing encompasses a wide range of attributes such as metallurgical state of alloy (composition, strength level, texture, residual stress history in fabrication), in-reactor stress intensity, iodine concentration, oxide layer type and thickness, and irradiation conditions [7]. Iodine escapes from the fuel to the highly radiolytic fuel-sheathing gap through diffusion or thermal cracking and is proportionate to the fission gas release [8].

Iodine isotopes are about 15% of the total U-235 fission isotopes [9]. Both iodine and ZrI_4 are serious ISCC initiating species for Zircaloy-4 [10]. To affect PCMI cracking from the interior, it is generally accepted that volatile fission by-products must be present locally and be above a threshold concentration [11]. The iodine concentration is highest in the fuel-sheathing gap [12], inducing a subsequent deleterious effect on the mechanical strength of the Zircaloy sheathing [4] [13]. High local iodine concentrations are reported on the sheathing at pellet crack locations [14]. Critical iodine concentrations for causing ISCC were tabulated earlier [15].

The main factor influencing ISCC is the chemical composition of Zircaloy sheathing, culminating in changes in the structure, mechanical and physical properties of the alloy system. The changes in strength and resulting resistance to ISCC are the primary by-products of the Zircaloy chemical makeup [16]. The experimental data and analyses [17] [18] have correlated the texture of non-irradiated Zircaloy-4, more than its chemical composition (for variations within the ASTM specification), with a strong effect on ISCC. The in-reactor structural integrity such as yield strength, fatigue and SCC are strongly correlated with the characteristic final texture in the finished Zircaloy sheathing product. The texture is affected by the tool design as well by the tube reduction parameters [19]. This further reinforces a conclusion that the Zircaloy tube manufacturing process is a significant factor in ISCC [20]. Residual stresses in materials arise in not only operational use, but stem from many a priori mechanical manufacturing and processing methods involving material deformation, heat treatment and machining. Almost every step of many machining processes can induce a wide variety of residual stresses with beneficial or detrimental effects. Particularly, the introduction of subsurface residual stresses in these operations, in terms of their depth, sign and magnitude may be the most influential factor in fatigue life, dimensional stability, brittle fracture and corrosion resistance. Since residual stresses are in self-equilibrium, both positive tensile, and negative compressive values must exist if residual stresses are present. These can be uniaxial, biaxial, or triaxial [21] [22].

Seamless Zircaloy-4 sheathing in CANDU reactors are manufactured in an incremental compression forming process called pilgering, where the sheathing tube is subject to a complex stress system. These stresses are not necessarily subject to continuous quality control assessment and monitoring, and unfortunately, in too many cases, residual stresses and their potential to improve or damage components subjected to repeat load cycles may be overlooked, or it is assumed that additional treatment either has eliminated them or introduced beneficial compressive stresses. The residual stresses persist as long as the sum of residual stress and applied external stress does not exceed the pertinent 0.2% yield stress ($\sigma_{y0.2}$) of the materials. The stresses required to cause SCC are small, usually below the macroscopic $\sigma_{y0.2}$, and are tensile in nature. When superimposed to repeated applied external stresses, residual stresses at the proper surface play a crucial role in the structural integrity of components and structures [22] [23]. This is critical in the nuclear field, where highly favourable (sub)surface residual compressive stresses in the Zircaloy sheath-

ing, efficiently retard the applied PCMI loading and overcome formation and propagation of cracks, thus enhancing fatigue resistance. Whereas residual tensile stresses are generally harmful and decrease the SCC resistance. Adequate depth and magnitude of the compressively stressed layer is important, in order to mitigate the initiation of cracks. Corrosion fatigue is often considered a subset of SCC [23]. During normal operations, high thermal conductivity in the fuel and sheathing, in conjunction with high sheathing strength and adequate creep resistance in the latter components are desired to withstand stress buildup in the sheathing [24]. Creep is deformation occurring as a constant volume process, normally at low stresses below the usual yield strength ($\sigma_{y0.2}$). Detailed thermo-mechanical analysis was able to show that during slow power ramping the sheathing and the pellet will creep, reducing the stress state of the former [25].

Zircaloy failure under the ISCC regime emerges from PCMI conditions, when the synergy of existing tensile hoop stress and stress imposed on the sheathing by fuel thermal expansions during steep power ascension rates, and corrosion reaction by high iodine concentration at the inner surface, are combined in tandem [4] [26] [27]. Initially, ISCC cracks proceed along the grain boundaries, and then propagate across the grains to leave a fracture pattern as a rupture during the ISCC process [4]. PCMI conditions and the associated ISCC process, as a by-product of sudden power ramping, can limit the lifetime and safety of the Zircaloy-4 sheathing [1]. Zircaloy sheathing has demonstrated a high probability of brittle fracturing due to PCMI, during severe power ramping in test reactors [28] and water-cooled reactors [29]. Ramp rates above 3% hour^{-1} [30] in fuel rods with extended service life over 10 GWd·t(U)$^{-1}$ [31], culminate in increased UO_2-pellet thermal expansion. The ensuing aggressive fission-gas product accumulation above a threshold concentration [11] [32] [33] and gap closure, generates local tensile hoop stresses on the inner surface of the sheathing, near radial fuel cracks or pellet-pellet interfaces [8] [34], at or above a stress threshold value. A sudden power increase that sets up such magnification of stresses plays a key role in the creation of PCMI conditions, normally leading to crack growth and failure in detectable ISCC. The crack propagates in the radial direction under a hoop stress. Crack growth rate has been expressed as a function of stress intensity [35]. The stress state in the sheathing then becomes a direct function of UO_2-pellet swelling during large power transitions, with higher burnups, therefore increasing the tensile stress state of the former [4] [36]. The burnup trials at 20 GWd·t(U)$^{-1}$ at the Bruce Power Reactor (Tiverton, ON) revealed a high failure rate due to PCMI conditions [32] [37]. Dynamic operations can cause considerable strains in CANDU fuel sheathing. For instance, the minimum strain predicted to initiate SCC cracking (0.1% - 0.5% [38]) is generally exceeded during power ramping in CANDU fuel, wherein the hoop strain in the sheathing can reach values of 0.8% - 1.3% and drop by 0.6% during a shutdown condition. Furthermore, the highest strains occur at fast ramp rates (1 kW·m^{-1}·min^{-1}), because they reduce the time available for fuel densification [39]. Under a power ramp regime, PCMI is minimized with high

strength sheathing and its ability to accommodate pellet expansion via creep, to delay sheathing ballooning and burst [40]. Threshold values of stress [41], stress intensity factor, iodine concentration for detectable ISCC [42], and iodine levels of PWR rods at normal and high burnups [43] [44] have been documented. A surplus of iodine over cesium reaches the sheathing in a power ramp [45] but is independent of fuel burnup [33].

PCMI conditions and the resulting ISCC failures remain a licencing concern for water reactors, including CANDU reactors, accommodating a multitude of power manoeuvrability events, higher discharge burnups and non-standard fuel designs, in a less conservative and more financially incentivized state of operation [3]. Although PCMI/ISCC mechanism accounted for very isolated failure rates of Zircaloy sheathing in all Pressurized Heavy Water Reactors (PHWR) surveyed during 2006-2015 [46], new safety requirements now include consideration of the effects of power cycling at high burnups [47], and development of reliable sheathing to mitigate PCMI conditions under these operating parameters [48]-[50]. The stresses induced by dynamic thermo-mechanical equilibrium under a PCMI scenario amplifies the fact that residual stress state of the sheathing above a certain threshold is highly correlated to the failure in SCC process. Residual compressive stresses protect the integrity of sheathing material from PCMI related ISCC, whereas residual tensile stresses promote ISCC in tests of Zircaloy in iodine vapors at 300˚C [51]. The Cold-Worked, Stress-Relieved (CWSR) microstructure and texture for CANDU fuel sheathing have been better controlled in the ensuing decades [52].

Multitude of obstacles inherent with in-reactor PCMI tests, have prompted considerable efforts in simulation of these conditions in the laboratory [26] [53]-[55]. A variety of different sample geometries have been examined (C-ring, standard tensile samples, and tube sections) using different methods for inducing stress (internal pressure tests, expanding mandrels, tensile and compression tests). Stress-Corrosion Cracking (SCC) in Zircaloy-4 fuel sheaths has previously been investigated by static loading of slotted ring samples [51] [56] [57]. At 300˚C, slotted Zircaloy rings crack in iodine vapour at applied hoop stresses greater than 217 MPa, where the failure time depends critically on whether the iodine concentration exceeds 3 mg $I_2 \cdot cm^{-2}$ of Zircaloy material [51]. In addition, the applied stress continuously relaxes during the test, which means that the stress could decay below the threshold stress for SCC during a long incubation period. These are disadvantages that make interpreting results difficult [4]. PCMI models provide reasonable failure predictions at low sheathing stresses (<1%) in test ramp data. In situations when fission product release is significant [58], general sheathing stresses are maintained well below yield by creep relaxation. In contrast, fuel rod codes that treat PCMI as a predominantly mechanical interaction [59] must resort to the assumption of unrealistically large stress concentration factors from the fuel pellet in order to raise the sheathing stress to its 0.2% yield strength ($\sigma_{\gamma 0.2}$) failure limit.

ISCC is not the dominant mode of failure for CANDU reactors. Improved re-

actor operating procedures to preclude severe power ramps, in addition to the introduction of CANLUB graphite coating used exclusively in CANDU reactors to protect Zircaloy-4 fuel sheathing [57], have been the cornerstone of reliability of power generation in Canada. Although a comprehensive review of ISCC processes has been presented earlier [60], a detailed examination of the most recent literature reveals the noticeable absence of ISCC investigations pertaining to the post-production stress history of Zircaloy-4, prior to the experimental undertaking in this work.

The test programme described here has primarily focused on determining the dependency of PCMI-ISCC on inherent residual stress within a wide range of non-irradiated, stress-relieved commercially available CANDU Zircaloy-4 sheathing and ubiquitous influence of iodine. A historical context is provided in terms of Zircaloy-4 sheathing from two independent sources, and their associated post-production stress state. In a first study of its kind, a more defining relationship between ISCC and the nature and magnitude of indigenous residual stress and the resulting changes in the mean stress to a constant hoop tensile stress, at or near the maximum 0.2% yield strength ($\sigma_{y0.2}$) of 400 MPa, by static loading of slotted Zircaloy-4 ring samples in corrosive conditions in iodine-methanol has been investigated.

2. Experimental Methods

2.1. Classic C-Ring Experimentation

CANDU-type tubes used in this study were Zircaloy-4 sheathing (diameter = 13.10 ± 0.05 mm; thickness = 0.39 ± 0.05 mm; length ≈ 490 mm). Two different lots of commercially available Zircaloy-4 sheathing samples, each with diverse production vintage have been independently sourced from their manufacturers, under very strict confidentiality agreements. All information regarding their source, exact chemical composition, and manufacturing process remains proprietary, and therefore unknown to the authors, henceforth referred to as Zr-*alpha* and Zr-*beta*. The as-received cold-worked stress-relieved, un-irradiated, non-hydrided Zircaloy-4 tubes, were sectioned into slotted Zircaloy-4 rings using a Buehler Isomet 1000 precision saw containing a circular diamond blade (151-mm-diameter). This process eliminates overloading the cutting force, therefore minimizing sample stress by means of a gravity-fed thin (0.4 mm) precision low-speed saw with IsoCut coolant, ensuring an exact and delicate sectioning with highest sample-to-sample consistency, in low-deformation radial cutting of narrow rings (5.00 ± 0.05 mm). This was followed by axial slitting to effect slot openings. The resulting C-rings were then sonicated in ethanol for 20 minutes to eliminate metal shavings and dust. After drying, the slotted C-rings were weighed (±0.02 mg). Scanning Electron Microscopy (SEM) examination, at sufficiently high magnification, was used to determine the positive initial slot openings in the C-rings. The C-rings' openings were imaged on a Quanta 250 FEG ESEM. The openings were manually measured using the line-measuring tool. The 88 samples comprised of 40 and 48 C-rings for Zr-*alpha* and Zr-*beta*, respectively.

2.2. Elastic Stress in a Slotted Zircaloy-4 C-Ring

Deflection Measurements

The deflections of slotted Zircaloy-4 rings were measured using a Class-1 precision lever system (**Figure 1**) [61]. A mass-load force exerted on one side will elevate a lever jaw on the opposite side to increase the slot size of the slotted ring, which is suspended over the lever jaw and a static jaw. For a slotted ring of known radius and axial length the slot deflection is proportional to the mass-load force and radius cubed, inversely proportional to mechanical strength (via Young's modulus), and to the ring thickness cubed [61]. Therefore, increases in the radius and decreases in thickness of slotted rings caused by corrosive processes, e.g., can be detected sensitively using this technique.

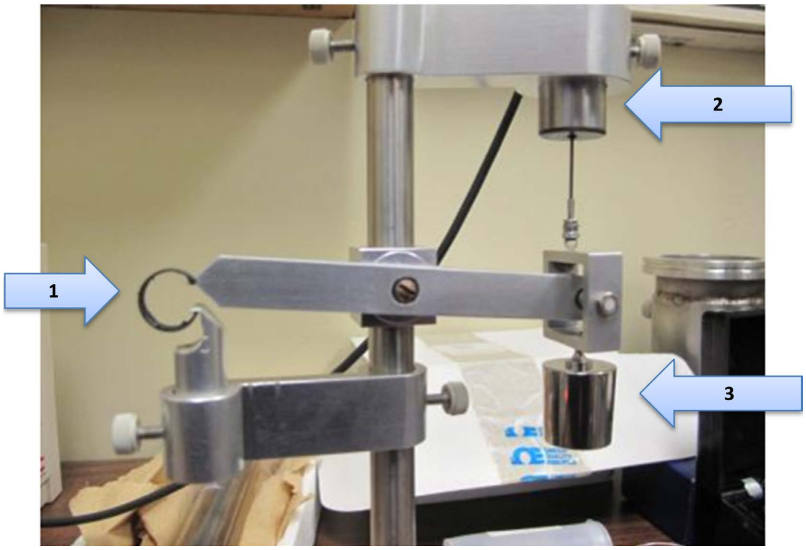

Figure 1. Deflection of slotted C-ring in a Class-1 precision lever system subject to 100.00 ± 0.01 g mass-load force [61]. C-ring (1), Linear displacement transducer (2), 100 g weight (3).

The rings were individually mounted on the apparatus and subjected to a fixed mass-load of 100.00 ± 0.01 g, in succession. A linear Omega LD400 series displacement transducer measures the ring deflection, which is captured by a LabVIEW™ program in real time. The lever jaw is continually maintained within ±0.0004 mm precision by calibration, after each measurement. The kinetic frictional force remains constant for all slotted rings throughout the measurements. After each deflection test, the unloaded slot opening was re-measured to verify that mass-load (100.00 ± 0.01 g) induced mainly elastic deformation.

SCC occurs beyond a threshold stress, and most likely initiates in regions of maximum stress. For the slotted ring geometry (**Figure 2**), the maximum stress occurs on the inner surface directly above the slot (*i.e.*, point *A*, **Figure 2(a)**). When the slot is stretched from its initial opening (w_0) to a final opening (w), the analytical formula for maximum stress (σ_A) vs. the half-angle (α, see **Figure 2(a)**) is [62]:

$$\sigma_A = \frac{Et(w-w_0)(1+\cos\alpha)}{2R^2\{(\pi-\alpha)(1+2\cos^2\alpha)+1.5\sin 2\alpha\}} \quad (1)$$

This formula for bending stress applies when the ring is elastically loaded. The ring has a radius (R = 6.55 mm), thickness (t = 0.39 mm), and a Young's modulus (of as-received Zircaloy-4 fuel sheath) given by [63]:

$$E = 97.83 - 0.0657(T - 273) \quad (2)$$

At room temperature (T = 296 K), the Young's modulus is 97.5 GPa. Typically, the half-angle is approximately 11˚ (= 0.19 rad), corresponding to the initial slot opening. As the half-angle approaches zero, Equation (1) simplifies to [64]:

$$\sigma_A = \frac{Et(w-w_0)}{3\pi R^2} \quad (3)$$

For the practical range of α values, the maximum elastic stress calculated in a COMSOL Multiphysics (version 4.4) finite element analysis model shows excellent agreement with Equation (1). In addition, the COMSOL model calculates the distribution of stress in the ring (**Figure 2(b)**) and helps to determine when shape variations cause Equation (1) to deviate from the true stresses in the ring. Furthermore, the COMSOL model can be modified to accommodate inevitable plastic and thermal stresses. Moreover, it can predict the surface strains caused by increasing the total gap deflection ($w-w_0$).

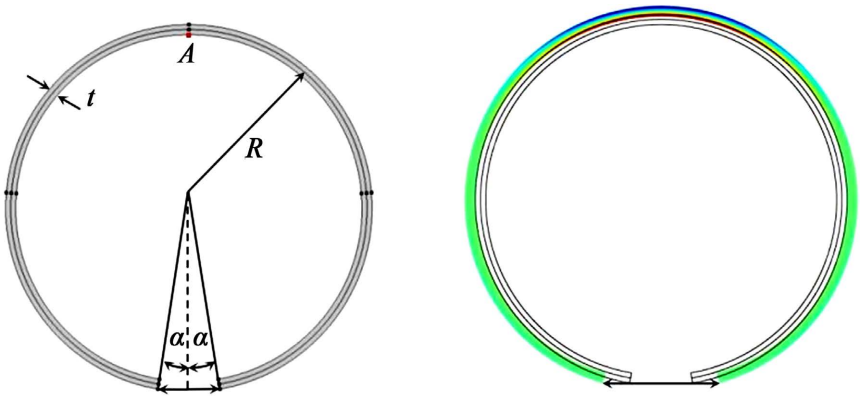

Figure 2. Slotted ring geometry (a): Equation (3) parameters, (b): acquiring a distribution of hoop stress (σ_x); colour plot indicates compressive stress (blue), tensile stress (red), and unstressed ring (green) [65].

2.3. PCMI and 0.2% Yield Strength ($\sigma_{y0.2}$)

The typical hoop stress in CANDU reactors fuel sheathing is generally below 100 MPa. This stress is primarily due to the internal pressure of fission gases and the thermal expansion of the fuel within. For a 1 mm total gap deflection ($w-w_0$) increase (Equation (3)), the COMSOL model predicts maximum strain and stress increases by approximately 0.10 % and 104 MPa, respectively. The maximum

0.2% yield strength ($\sigma_{y0.2}$) for non-irradiated, stress-relieved Zircaloy-4 sheathing lies within 414 - 565 MPa (at room temperature), depending on metallurgical conditions [66]. This corresponds well to the range of strains induced by severe power ramps in CANDU nuclear reactors (0.8% - 1.3%) [39] and exceeds the minimum strain range for inducing SCC in Zircaloy-4 sheathing (0.1% - 0.5%) [17]. Purely elastic deflection of C-rings is expected only up to 300 MPa [67]. Beyond 300 MPa, plastic stress will begin contributing to the overall stress. For constant pressure, the maximum hoop stress at which ISCC was observed was around 400 MPa. Above that value, failure did not occur via ISCC. The lower threshold stress, below which failure by ISCC did not occur, was around 240 MPa for all the loading modes, before 72 h [68]. Consequently, static hoop tensile stress tests in this study were conducted with stresses applied around 400 MPa (σ_A; Equation (3)). Although fuel sheathing is subject to equibiaxial stress conditions during a power ramp, practical laboratory tests for SCC of Zircaloy-4 sheathing are performed by uniaxial constant load hoop tensile stress (axial stress = 0). Under conditions of a near equibiaxial stress state, SCC of Zircaloy in an iodine-bearing medium occurs more rapidly than due to uniaxial loading [69].

Significant differences with in-reactor environment notwithstanding, C-ring geometry subject to a uniaxial static hoop tensile stress, in an iodine-methanol medium at room temperature, allows for accurate control of mechanical and chemical stress environment in reproduction of cracking and fracture conditions in this study. Specimens of Zircaloy-4 in an iodine-methanol medium without applied load fail in several days; after loading by uniaxial tension, the specimens fail in several hours [70]. Iodine-methanol medium replicates fracture processes in iodine vapours very closely. Fractures obtained in internal pressure tests for SCC in iodine vapors at $T = 350^{\circ}C$ and in an iodine-methanol medium at room temperature are largely identical [70]. Iodine forms complex compounds with alcohols, where one molecule of the alcohol is bonded to one iodine atom. The size of the alcohol molecule is minimum in the case of solution of iodine in methanol. Therefore, the sensitivity of Zircaloy to SCC in a solution of iodine in methanol is higher than in solutions of iodine in other alcohols [71]. The latter is associated with steric hindrance of higher molecular weight alcohols decreasing the rate of intergranular corrosion and the resulting SCC susceptibility of Zircaloy-4 [71].

2.4. Zircaloy-4 C-Rings in a Stress-Corrosion Test Environment

Individual Zircaloy-4 C-rings from Zr-*alpha* and Zr-*beta* series were mechanically loaded by a uniaxial constant load hoop tensile stress in the form of a rectangular Polyether Ether Ketone (PEEK) block. A schematic diagram of this arrangement is shown in **Figure 3**. The ease of processing, superior wear resistance and strength, and formidable chemical resistance, form the foundation of choosing this novel material as a mechanical wedge.

The PEEK wedge blocks were individually precision-machined (6.40 - 10.00 ± 0.01 mm) to deliver a constant hoop tensile stress of 400 (±2%) MPa [68] for each

C-ring, caused by increasing the total gap deflection ($w - w_0$) in Equation (3). Post-deflection geometric radius (R) in the latter equation was then determined (±0.01 mm) by integration of the initial slot opening and the wedge block specific to each slotted ring with the original radius of 6.55 mm. Since Zircaloy-4 under uniaxial tension, in an iodine-methanol medium, fails in hours [70], the mechanically wedged C-ring samples in this study were submerged in a 30 mL glass of freshly prepared iodine-methanol solution (10 g/1000mL) [71] at room temperature for 4.0 hours. The high iodine concentration is not representative of iodine concentration in the fuel-sheathing gap [12]. Anhydrous methanol (water < 0.01%) and iodine (99.9%) were used in this study. After emerging from iodine-methanol solution, the wedged C-rings were immediately rinsed in fresh methanol repeatedly. Subsequently, the wedges were dismounted uniaxially, and the C-rings were allowed to dry. All samples were re-weighed (±0.02 mg) and the surviving C-rings that did not suffer complete fracture failure and splitting, were re-examined under SEM for the resulting corrosion effects.

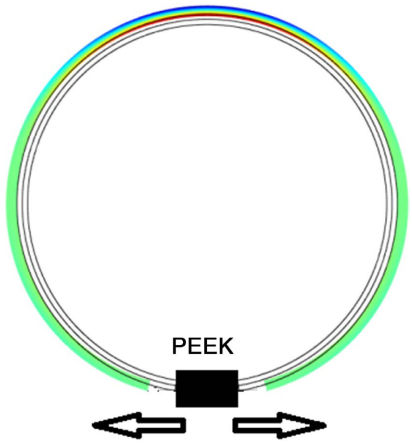

Figure 3. Zircaloy-4 C-Ring mechanically loaded by a uniaxial constant load hoop tensile stress in the form of a rectangular Polyether Ether Ketone (PEEK) block.

3. Results

3.1. Determination of Original Residual Stress in Zircaloy-4 C-Rings

The initial slot openings in narrow Zircaloy-4 C-rings (5.00 ± 0.05 mm), from Zr-*alpha* and Zr-*beta* series, were captured by Scanning Electron Microscopy (SEM). Maximum and minimum displacements in the form of positive slot openings as a result of axial slitting range between 0.9173 and 0.4155 mm for Zr-*alpha* series. In Zr-*beta* series, the maximum and minimum positive slot openings are 2.525 and 0.4371 mm. The results of SEM measurements of positive slot openings (mm) for rings from Zr-*alpha* and Zr-*beta* series are displayed in **Figure 4** and **Figure 5**, respectively. Individual measurements (±0.0004 mm) presented are the average of 4 measurements for each vintage year, batch and the tube sample number. The average positive slot opening for Zr-*alpha* series is 0.5576 (±0.0525) mm. This is

in clear contrast to the higher average positive slot opening of 1.009 (±0.364) mm for the Zr-*beta* series, in addition to a much larger scatter in the vintage years studied. A quantitative relationship between the positive initial slot openings ($w - w_0$), based on individual SEM measurements, allows for determination of

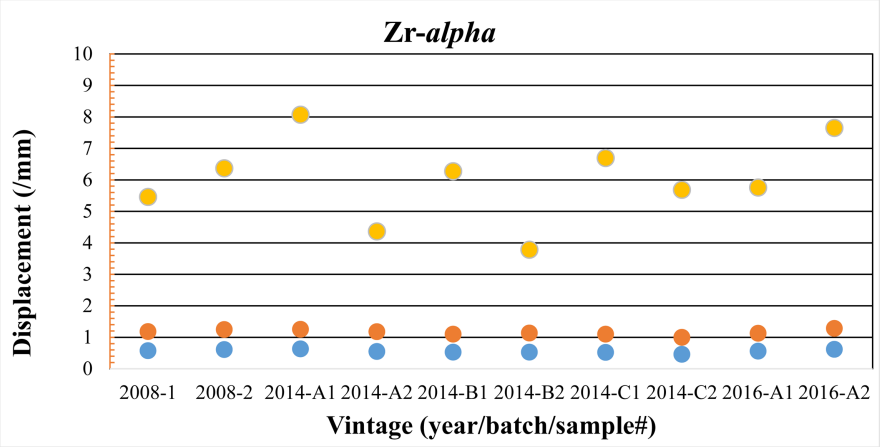

Figure 4. Initial slot openings of narrow C-rings (5.00 ± 0.05 mm) after axial slitting, and total deflections post mass-load force (100.00 ± 0.01 g) in a Class 1 lever system (**Figure 1**). Slot openings post iodine-methanol Stress-Corrosion trials (400 (±2%) MPa). All data is the average of 4 measurements (±0.0004 mm). Zr-*alpha* slotted C-ring vintage year, the batch (A, B and C), and tube sample (1 and 2).

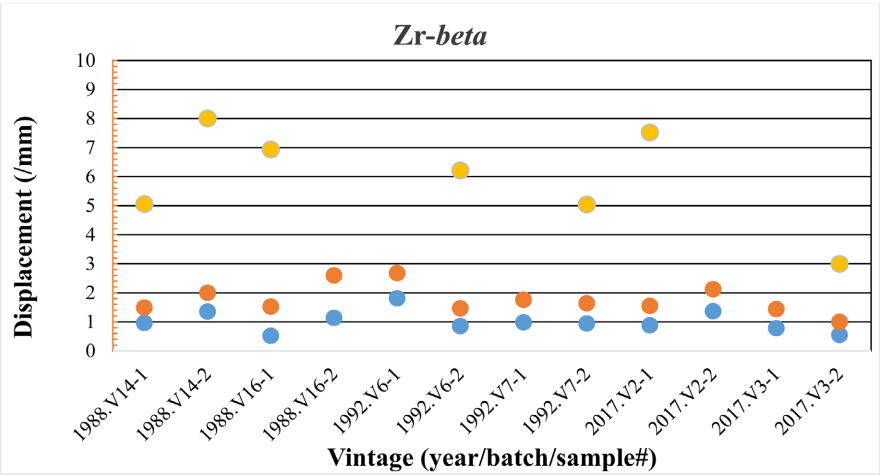

Figure 5. Initial slot openings of narrow C-rings (5.00 ± 0.05 mm) after axial slitting, and total deflections post mass-load force (100.00 ± 0.01g) in a Class 1 lever system (**Figure 1**). Slot openings post iodine-methanol Stress-Corrosion trials (400 (±2%) MPa). All data is the average of 4 measurements (±0.0004 mm). Zr-*beta* slotted C-ring vintage year, the batch (V), and tube sample (1 and 2). Fractured C-ring sample groups are indicated by missing data points.

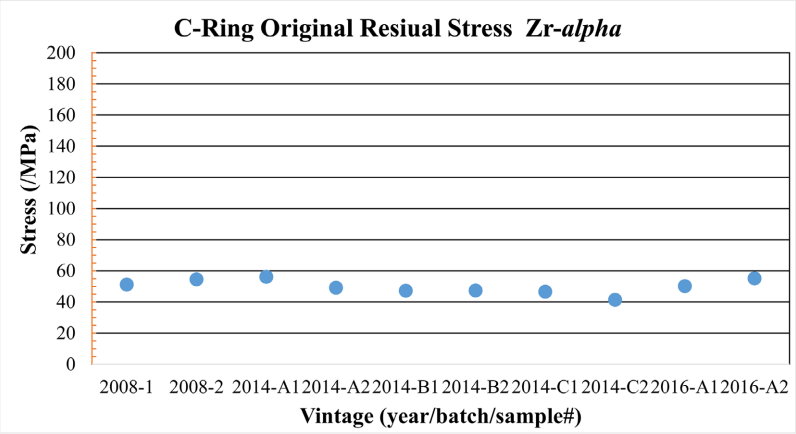

Figure 6. Tensile residual stresses based on SEM measurements of the initial slot openings for C-rings from Zr-*alpha* series (Equation (3)). All data is the average of 4 measurements. Zr-*alpha* slotted C-ring vintage year, the batch (A, B and C), and tube sample (1 and 2).

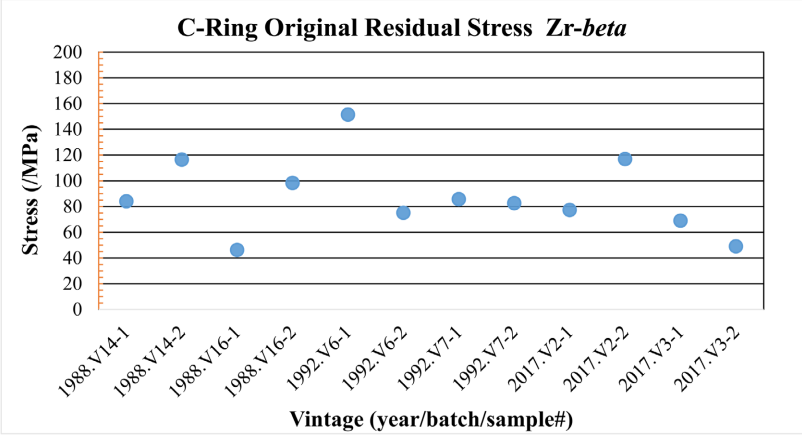

Figure 7. Tensile residual stresses based on SEM measurements of the initial slot openings for C-rings from Zr-*beta* series (Equation (3)). All data is the average of 4 measurements. Zr-*beta* slotted C-ring vintage year, the batch (V), and tube sample (1 and 2).

the residual tensile stresses (σ_A) for individual C-rings from Zr-*alpha* and Zr-*beta* series (Equation (3)) [64]. The latter equation incorporates the ring radius (R = 6.55 mm), thickness (t = 0.39 mm), and a Young's modulus (of as-received Zircaloy-4 fuel sheath (Equation (2)) [63]; 97.5 GPa) as constants in the determination of residual tensile stresses. The average of 4 residual tensile stresses (MPa) for each vintage year, batch and the tube sample number are presented in **Figure 6** and **Figure 7** for Zr-*alpha* and Zr-*beta* series, respectively.

A statistical examination of initial residual tensile stress data for Zr-*alpha* and Zr-*beta* C-ring series appears in **Table 1**. The Zircaloy-4 sheathing tubes from Zr-*alpha* series clearly exhibit a lower group average residual tensile stress (49.84 MPa), incorporating a substantially lower scatter (±4.55 MPa) across the vintage years examined. This is further amplified by comparatively the lowest average maximum tensile stress value of 56.10 MPa in a vintage year and batch (2014-A1). The higher group average of 87.63 MPa and the highest average maximum value

of 151.41 MPa, in a vintage year and batch (1992.V6-1), exemplify the measurably higher residual tensile stresses in the Zr-*beta* sample series, in addition to the much larger scatter (±29.75 MPa) in the vintage years under examination. The Coefficient of Variance of residual tensile stresses for Zr-*alpha* and Zr-*beta* series measures 9.13% and 33.95%, respectively. Additionally, the two-sample *t*-test with the confidence interval (S = 0.95; $\alpha = 0.05$) for the difference between the means of the original residual tensile stress in Zr-*alpha* and Zr-*beta*, and their associated standard deviations, provides a significant and compelling case for the inferiority of Zr-*beta* in its inherent residual tensile stress.

Table 1. Residual tensile stress data for Zr-*alpha* and Zr-*beta* C-ring series across all vintage years.

Residual Tensile Stress (MPa)	Zr-*alpha*	Zr-*beta*
Number of Samples	40	48
Average	49.84	87.63
Median	49.64	83.27
Standard Deviation	4.55	29.75
Coefficient of Variation (%)	9.13	33.95
Maximum Value	56.10	151.41
Minimum Value	41.34	46.18

The deflection behaviour of Zircaloy-4 C-rings is investigated (Section 2.2.1) in a Class-1 precision lever system subject to 100.00 ± 0.01 g mass-load force (**Figure 1**) [61]. Total deflections post mass-load force, are contrasted against the initial slot openings of Zr-*alpha* and Zr-*beta* series in **Figure 4** and **Figure 5**, respectively. After the removal of mass-load force, the self-reversing of the slot openings to <±0.0008 mm (not shown in **Figure 4** and **Figure 5**) of the initial slot openings, validates the purely elastic nature of deformation for both Zr-*alpha* and Zr-*beta* series.

3.2. Results of SCC of C-Rings Stressed at 400 MPa in Iodine-Methanol

Section 2.4 details the Zircaloy-4 C-Rings trials in a Stress-Corrosion Test Environment. Mechanically loaded (400 (±2%) MPa) C-rings from Zr-*alpha* series did not suffer any fracture failure in the Stress-Corrosion trial in the high iodine concentration, methanol medium (10 g/1000mL) at room temperature (**Figure 4**). C-rings from Zr-*beta* series suffered fracture failure, spread across the vintage years (1988-2017), batch and samples, resulting in complete splitting of the C-rings into two sections, under exactly similar Stress-Corrosion conditions. The latter failed C-ring sample groups are indicated by missing data points in Stress-Corrosion trial results in **Figure 5**. All data is the average of 4 measurements (±0.0004 mm), for each vintage year, batch and the tube sample number. The failed C-rings from

Zr-*beta* series notwithstanding, the resulting average slot openings emerging from Stress-Corrosion trials is 6.009 mm (±1.322) for Zr-*alpha* series, and 5.963 mm (±1.791) for Zr-*beta* series. Figure 8 shows SEM images of representative slotted Zircaloy-4 C-ring openings from the two sources after emerging from iodine-methanol Stress-Corrosion trial.

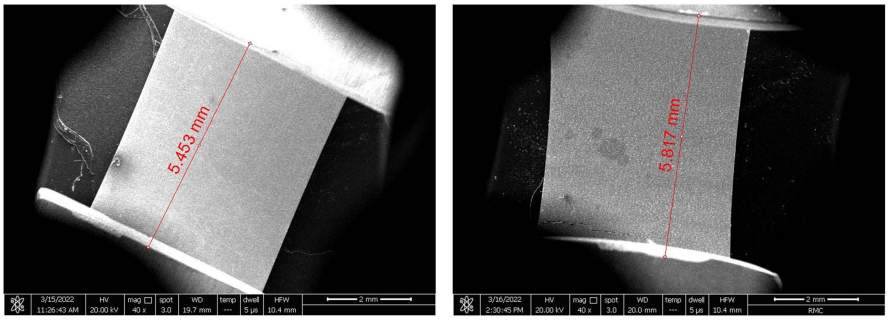

Figure 8. Representative slotted Zircaloy-4 ring openings from Zr-*alpha* (R: 5.817 mm) and Zr-*beta* (L: 5.453 mm) after emerging from iodine-methanol Stress-Corrosion trial.

The slotted Zircaloy-4 C-rings were weighed (±0.02 mg) prior and post Stress-Corrosion trials. A group average for Zr-*beta* series that did not suffer complete fracture failure, resulting in splitting of the C-ring into two sections in the Stress-Corrosion trial, showed a 1.71% weight loss as compared to a 0.90% weight loss for a group average for Zr-*alpha* series.

Zr-*alpha* series comprised of 40 C-rings displayed varying extents of post ISCC effects, ranging from complete absence of cracking in the inner surface to intergranular ISCC cracking (Figure 9), and did not suffer any fracture failure (Figure 4). However, C-rings from Zr-*beta* series suffered fracture failure spread across the vintage years (1988-2017), batch and samples, resulting in complete splitting of the C-ring into two sections. The five failed groups of Zr-*beta* samples comprised of 20 C-ring samples (Figure 5; missing data points), of the total 48 Zr-*beta* series. The remainder Zr-*beta* samples shared varying extents of post ISCC effects ranging from agglomeration of pits, intergranular cracking, and ductile fracture failure (Figure 10).

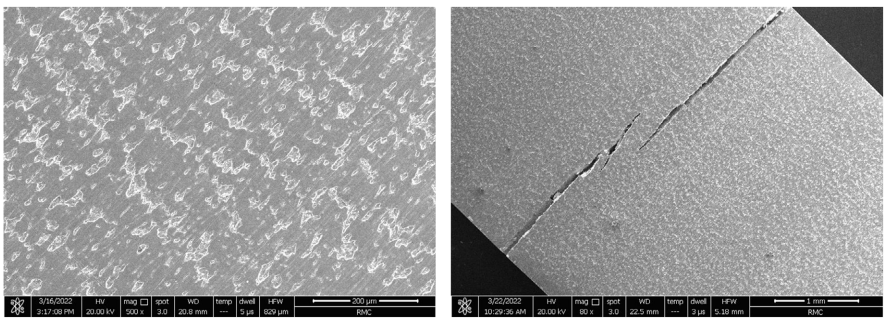

Figure 9. SEM Images of lower residual tensile stress Zr-*alpha* C-ring samples post Stress-Corrosion trial diametrically across the slot zone (*i.e.*, point *A*, Figure 2(a)). Complete absence of cracking in the inner surface (L: mag. ×500) and cross-section of the intergranular ISCC cracking (R: mag. ×80).

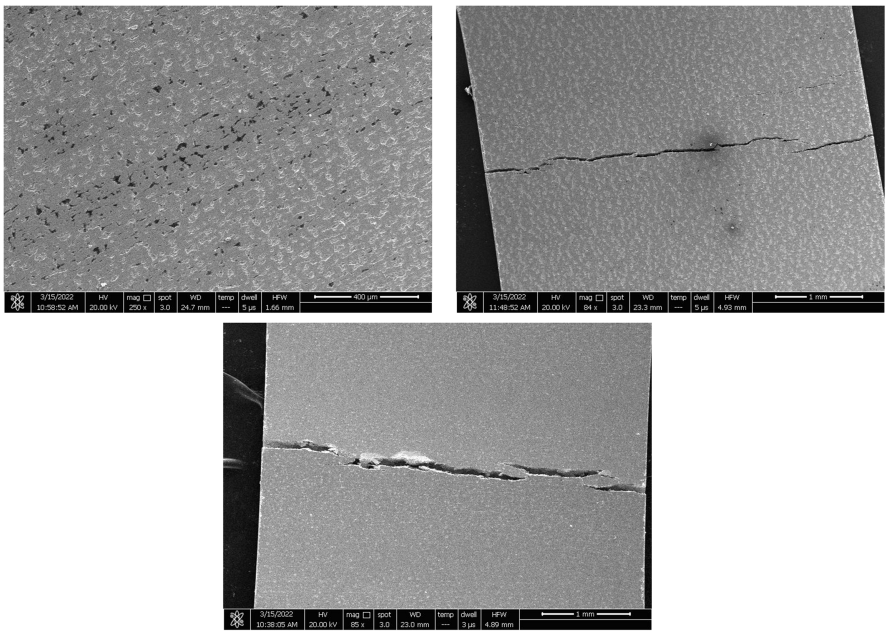

Figure 10. SEM images of higher residual tensile stress Zr-*beta* C-ring samples post Stress-Corrosion trial diametrically across the slot zone (i.e., point *A*, **Figure 2(a)**). Various cross sectional ISCC effects (top to bottom) ranging from agglomeration of pits (mag. ×250), intergranular cracking (mag. ×84), and ductile fracture (mag. ×85).

4. Discussion

The axial slitting to effect slot openings in narrow rings (5.00 ± 0.05 mm), releases the residual stress distributed relatively uniformly in the entire length of the original Zircaloy-4 sheathing (≈490 mm). A quantitative relationship between the slot opening and residual stress has been formulated (Equation (3)) [64], based on the elasticity of the slotted C-ring. The purely elastic deflection behaviour of the C-rings is verified for before and after the fixed mass-load (100.00 ± 0.01 g), in the Zr-*alpha* and Zr-*beta* C-ring series, respectively. The displacement in the form of positive slot openings (**Figure 4** and **Figure 5**) is categorically predictive of the universal presence of hoop tensile stress in the rings. Residual tensile stress data for Zr-*alpha* and Zr-*beta* C-ring series (**Figure 6** and **Figure 7**) were quantitatively determined (Equation (3)) [64] prior to Stress-Corrosion trials. Zr-*alpha* series incorporate residual tensile stresses of 49.84 ± 4.55 MPa across the vintage years 2008-2016. For Zr-*alpha* series, coefficient of variation of 9.13%, from a production and quality control management process, reflects lower dispersion and highly consistent residual stress properties [72], and hence the ability to effectively combat the fuel sheathing failure for various reactor conditions (e.g., power ramps, increased linear power, etc.), and to further support higher burnups in advanced fuel cycles [56] [73]. This is further amplified by comparatively the lowest average maximum tensile stress value of 56.10 MPa in a vintage year and batch (**Figure 6**; 2014-A1). This is in clear contrast to quantitatively higher average post-production residual tensile stress of 87.63 ± 29.75 MPa for Zr-*beta* series across the vintage years 1988-2017. Zr-*beta* sample series integrate distinctively higher standard

deviation and resulting coefficient of variation of 33.95%, reflecting unfavourably high dispersion and inconsistent residual stress profile. The highest average maximum value of 151.41 MPa, in a vintage year and batch (**Figure 7**; 1992.V6-1), exemplify the measurably higher residual tensile stresses in the Zr-*beta* series. The higher average post-production residual tensile stresses inherently mask the riskiest cases in the Zr-*beta* series.

The depth and particularly the magnitude of post-production subsurface residual tensile stresses of Zircaloy-4 sheathing in CANDU reactors, manufactured in pilgering process, are influential in fatigue life, dimensional stability, brittle fracture and corrosion resistance. The synergy of existing higher residual tensile stress, and stresses at or near the maximum 0.2% yield strength ($\sigma_{y0.2}$) imposed on the C-rings are generally harmful and decrease the ISCC resistance [4] [26] [27]. The samples from Zr-*alpha* series comprised of 40 C-rings with decisively lower original residual tensile stresses of 49.84 ± 4.55 MPa across the vintage years (**Figure 6**), did not suffer a single fracture failure post 400 (±2%) MPa stress, in iodine-methanol solution at room temperature (**Figure 4**). C-rings prepared from Zr-*beta* series suffered fracture failure spread across the vintage years, resulting in complete splitting of the C-ring into two sections. The five failed groups from Zr-*beta* series comprised of 20 C-ring samples (**Figure 5**; missing data points), possessed the highest average original residual tensile stresses, ranging from 68.95 to 151.41 MPa, across all 88 samples from Zr-*alpha* and Zr-*beta* series (**Figure 6** and **Figure 7**). The latter values and the higher group average of 87.63 ± 29.75 MPa in the Zr-*beta* series, exemplify the measurably higher residual tensile stresses synonymous with larger mean stresses, resulting in cracking and fracture failure post 400 (±2%) MPa stress, in iodine-methanol solution at room temperature. The latter failed sample groups are indicated by missing data points in Stress-Corrosion trial results in iodine-methanol at 400 (±2%) MPa in **Figure 5**. Depending on metallurgical conditions, the aforementioned stress condition lies at or near the maximum 0.2% yield strength ($\sigma_{y0.2}$) for non-irradiated, stress-relieved Zircaloy-4 sheathing of 414 - 565 MPa [66].

Original post-production residual stress can raise or lower the mean stress experienced over a fatigue cycle. The Goodman relation is particularly helpful in determining the effectiveness of a material, because a residual tensile stress increases the mean stress [74]. Mean stress values incorporating higher residual tensile stresses are more likely to promote ISCC than residual compressive stresses. Larger mean stress values promote ISCC in tests of Zircaloy in iodine vapours at 300˚C [51] and may trigger static fracture during fatigue.

The Zr-*beta* sample series displayed the more pronounced post ISCC effects from pitting to ductile fracture (**Figure 10**), diametrically across the slot zone (*i.e.*, point *A*, **Figure 2(a)**). In contrast, the Zr-*alpha* sample series, with lower mean stresses, displayed the more mitigated post ISCC effects in the same zone, including the complete absence of cracking in the inner surface, and cracking without pitting (**Figure 9**). The iodine-methanol Stress-Corrosion medium had been ob-

served earlier as the most aggressive, in terms of penetration depth [71].

The resulting average slot openings post iodine-methanol Stress-Corrosion trials are 6.009 mm (±1.322) and 5.963 mm (±1.791) for Zr-*alpha* and Zr-*beta* series, respectively; the failed C-rings from Zr-*beta* excepted. This degree of experimental scatter is common in ISCC experimental campaigns, and the 0.77% difference between average slot openings between the two series amplifies the notion that iodine-methanol medium consistently replicates Stress-Corrosion effects. Fractures obtained in internal pressure tests for SCC in iodine vapors at T = 350˚C and in an iodine-methanol medium at room temperature are largely identical [70].

The slotted C-rings were weighed (±0.02 mg) prior and post Stress-Corrosion testing, during which the chemical as well as the mechanical conditions for cracking are satisfied [4] [75]. Zr-*beta* C-ring series possessing larger mean stress, that did not suffer complete fracture failure, registered a 1.71 % average weight loss as compared to a 0.90% weight loss for a group average for Zr-*alpha* series with lower mean stress. The extent of intergranular cracking is greater in statically loaded tests particularly for iodine solutions in organic solvents, resulting in dissolution, removal of material and larger weight loss during cracking from the grain boundaries [76]. Increasing the original slot openings for all C-rings in the range of 6.40-10.00 mm (Equation (3)) to deliver a constant hoop tensile stress of 400 (±2%) MPa, at or near the maximum 0.2% yield strength ($\sigma_{y0.2}$) for non-irradiated, stress-relieved Zircaloy-4 sheathing of 414 - 565 MPa [66], induces a strain between 0.7 to 1.1% [73]. This is comparable to the strains induced by power ramps in CANDU nuclear reactors (0.8% - 1.3%) [39] and exceeds the minimum strain range for inducing SCC in Zircaloy-4 sheathing (0.1% - 0.5%) [17]. During power ramps and increased linear power operations in water-cooled reactors, Zircaloy sheathing has demonstrated a high probability of brittle fracturing due to PCMI and associated ISCC process [29].

The positive slot opening remains purely a function of the individual post-production residual tensile stress (Equation (3)) [64] across the vintage year, batch and the tube sample number for Zr-*alpha* and Zr-*beta* series (**Figure 6** and **Figure 7**). In spite of the fact that axial slitting to effect slot openings may have relieved the original residual tensile stress to the largest extent possible, the unfavourably higher and irregular original residual tensile stress profile of Zr-*beta* series (87.63 ± 29.75 MPa) and associated mean stress of 400 (±2%) MPa, at or near the maximum 0.2% yield strength ($\sigma_{y0.2}$), are evidently manifested in Zr-*beta* series having suffered wide spread brittle fracture failure under the ISCC regime in this investigation. This would be potentially limiting the lifetime and safety of the Zircaloy-4 sheathing in power maneuverability events.

5. Conclusions

The positive initial slot openings, based on individual SEM measurements, allows for determination of the indigenous residual tensile stresses for individual C-rings from Zr-*alpha* and Zr-*beta* series. The Zircaloy-4 sheathing tubes from Zr-*alpha*

series clearly exhibit a lower group average residual tensile stress (49.84 MPa), incorporating a substantially lower scatter (±4.55 MPa) across the vintage years examined. The higher group average of 87.63 MPa, exemplifies the measurably higher residual tensile stresses in the Zr-*beta* sample series, in addition to the much larger scatter (±29.75 MPa) in the vintage years under examination. The Coefficient of Variance of residual tensile stresses for Zr-*alpha* and Zr-*beta* series measures 9.13% and 33.95%, respectively. Zr-*beta* sample series reflect unfavourably high dispersion and inconsistent inherent residual stress profile. The two-sample *t*-test provides a decisive case for the inferiority of Zr-*beta* in its inherent residual tensile stress.

It has been demonstrated that Zircaloy-4-based C-rings stressed at or near the maximum 0.2% yield strength ($\sigma_{y0.2}$) of 414 - 565 MPa [66], for non-irradiated, stress-relieved Zircaloy-4 sheathing, in iodine-methanol, subject to the original residual tensile stress and the resulting changes in the mean stress, are susceptible to Stress-Corrosion Cracking and fracture. The samples from Zr-*alpha* series composed of 40 C-rings with decisively lower original residual tensile stresses across the vintage years did not suffer a single fracture failure post 400 (±2%) MPa stress. In contrast, the 48 C-rings from the Zr-*beta* series suffered fracture failure spread across the vintage years, resulting in complete failure and splitting of 20 C-rings into two sections. Zr-*beta* C-ring series possessing larger mean stress, registered a 1.71 % average weight loss, reflecting a greater intergranular cracking as compared to a 0.90% weight loss for a group average for Zr-*alpha* series with lower mean stress.

The presence of higher residual tensile stress as a structural element in commercially available Zircaloy-4 has been established to considerably undermine corrosion resistance and enhance brittle fracture. The future advancement of Zircaloy sheathing production should embrace the stress state of the latter and its inevitable changes during reactor power transitions. Considerable advantage can be realized by engineering beneficial residual compressive stress in the sub-surface layers of the Zircaloy substrate to mitigate origination and propagation of deleterious Stress-Corrosion Cracking and increase wear resistance. It is noteworthy that the findings of this particular investigation are not exactly representative of Zircaloy-4 sheathing performance inside a CANDU reactor and complimentary studies incorporating sheathing condition properties like irradiation damage, oxide layer thickness, hydride concentration and a more superior siloxane coating, would further enhance the forecasting of sheathing behaviour in a reactor environment.

Highlights

- Subsurface residual stresses are present as a post-production structural element in commercially available Zircaloy-4 sheathing.
- Commercially available CANDU Zircaloy-4 fuel sheathing samples are stressed at or near the maximum 0.2% yield strength ($\sigma_{y0.2}$) of 400 (±2%) MPa in iodine-

methanol.

- The synergy of existing higher residual tensile stress, and stresses at or near the maximum 0.2% yield strength ($\sigma_{y0.2}$) in Zircaloy-4 fuel sheathing samples are generally harmful and confirmed to decrease the Iodine Stress Corrosion Cracking resistance.

Acknowledgements

Clarence McEwen, Senior Technologist, Department of Chemistry and Chemical Engineering, Royal Military College, Canada, precision-machined individual Polyether Ether Ketone (PEEK) blocks (6.40 - 10.00 ± 0.01 mm).

Funding

This work was partially funded by Natural Sciences and Engineering Research Council of Canada (NSERC-CRDPJ-436050-12).

Conflicts of Interest

The authors declare no conflicts of interest regarding the publication of this paper.

References

[1] Robertson, J.A.L. (1975) Proceedings of the Joint Topical Meeting on Commercial Nuclear Fuel Technology Today, Toronto, 28-30 April, 2.

[2] Rosenbaum, H.S., Davies, J.S. and Pon, J.Q. (1966) US Report GEQP-5100-5. https://www-pub.iaea.org/MTCD/Publications/PDF/te_1185_prn.pdf

[3] International Atomic Energy Agency (2000) Iodine Induced Stress Corrosion Cracking of Zircaloy Fuel Cladding Materials, IAEA-TECDOC-1185, IAEA, VIENNA.

[4] Cox, B. (1990) Pellet-Clad Interaction (PCI) Failures of Zirconium Alloy Fuel Cladding—A Review. *Journal of Nuclear Materials*, **172**, 249-292. https://doi.org/10.1016/0022-3115(90)90282-r

[5] Hellouin de Menibus, A., Auzoux, Q., Besson, J. and Crépin, J. (2014) Temperature Increase of Zircaloy-4 Cladding Tubes Due to Plastic Heat Dissipation during Tensile Tests at 0.1-10 S-1 Strain Rates. *Journal of Nuclear Materials*, **454**, 247-254. https://doi.org/10.1016/j.jnucmat.2014.08.011

[6] Knaab, H., Gartner, M. and Sontheimer, F. (1987) Proceedings of the IAEA Meeting on Pellet-Cladding Interaction and Load-Following Behaviour of Water Reactor Fuel, Lyon, 18-21 May 1987, Report No. IWGFPT/28.

[7] Piro, M.H.A., Sunderland, D., Livingstone, S., Sercombe, J., Revie, W., Quastel, A., Terrani, K. and Judge, C. (2017) A Review of Pellet-Clad Interaction Behavior in Zirconium Alloy Fuel Cladding. Ref. Modul. Mater. Sci. Mater. Eng, Elsevier.

[8] Garzarolli, F., Manzel, R., Peehs, M. and Stehle, H. (1978) *Kerntechnik*, **20**, 27-31.

[9] van der Schaaf, B. (1974) Fracture of Zircaloy-2 in an Environment Containing Iodine. In: *Zirconium in Nuclear Applications*, ASTM International, 479-494. https://doi.org/10.1520/stp32135s

[10] Cubicciotti, D., Jones, R. and Syrett, B. (1982) Chemical Aspects of Iodine-Induced Stress Corrosion Cracking of Zircaloys. In: Garde, A.M. and Bradley, E.R., Eds., *Zirconium in the Nuclear Industry*, ASTM International, 146-157.

https://doi.org/10.1520/stp37052s

[11] Peehs, M., Steinberg, E. and Stehle, H. (1980) Proceedings of the IAEA Meeting on Pellet-Cladding Interaction in Water Reactors, Risø, p. 169.

[12] Kleykamp, H. (1985) The Chemical State of the Fission Products in Oxide Fuels. *Journal of Nuclear Materials*, **131**, 221-246. https://doi.org/10.1016/0022-3115(85)90460-x

[13] Wimmer, E., Najafabadi, R., Young Jr, G.A., Ballard, J.D., Angeliu, T.M., Vollmer, J., *et al.* (2010) *Ab Initio* Calculations for Industrial Materials Engineering: Successes and Challenges. *Journal of Physics: Condensed Matter*, **22**, Article ID: 384215. https://doi.org/10.1088/0953-8984/22/38/384215

[14] Davies, J.H., Rosenbaum, H.S., Armijo, J.S., Rosicky, E., Esch, E.L. and Wisner, S.B. (1977) Proceedings of the ANS Topical Meeting on Water Reactor Fuel Performance, ANS, St. Charles, p. 230.

[15] Une, K. (1980) Threshold Values Characterising Iodine-Induced SCC of Zircaloys Obtained in Laboratory Experiments. *Proceedings of the IAEA Meeting on Pellet-Cladding Interaction in Water Reactors*, Risø, p. 226.

[16] Nikulin, S.A. and Rozhnov, A.B. (2005) Corrosion Cracking of Zirconium Cladding Tubes (A Review). I. Methods of Study and Mechanisms of Fracture. *Metal Science and Heat Treatment*, **47**, 71-79. https://doi.org/10.1007/s11041-005-0034-2

[17] Sidky, P.S. (1998) Iodine Stress Corrosion Cracking of Zircaloy Reactor Cladding: Iodine Chemistry (A Review). *Journal of Nuclear Materials*, **256**, 1-17. https://doi.org/10.1016/s0022-3115(98)00044-0

[18] Schuster, I. and Lemaignan, C. (1992) Influence of Texture on Iodine-Induced Stress Corrosion Cracking of Zircaloy-4 Cladding Tubes. *Journal of Nuclear Materials*, **189**, 157-166. https://doi.org/10.1016/0022-3115(92)90528-s

[19] Linga Murty, K. and Charit, I. (2006) Texture Development and Anisotropic Deformation of Zircaloys. *Progress in Nuclear Energy*, **48**, 325-359. https://doi.org/10.1016/j.pnucene.2005.09.011

[20] Garlick, A. and Wolfenden, P.D. (1971) Fracture of Zirconium Alloys in Iodine Vapour. *Journal of Nuclear Materials*, **41**, 274-292. https://doi.org/10.1016/0022-3115(71)90165-6

[21] Withers, P.J. and Bhadeshia, H.K.D.H. (2001) Residual Stress. Part 2—Nature and Origins. *Materials Science and Technology*, **17**, 366-375. https://doi.org/10.1179/026708301101510087

[22] Noyan, I.C. and Cohen, J.B. (1987) Residual Stress: Measurement by Diffraction and Interpretation. Springer, 1-46.

[23] Ricker, R.E. (1992) Chapter 1, Mechanisms of Stress Corrosion Cracking. In: Jones, R.H., Ed., *Stress-Corrosion Cracking, Materials Performance and Evaluation*, ASM International, 1-40.

[24] (2012) NEA Report No. 7072, Nuclear Fuel Safety Criteria Technical Review. 2nd Edition, Nuclear Energy Agency, OECD.

[25] Porrot, E., Charles, M., Lefebvre, F. and Lemaignan, C. (1988) Mechanisms of Cladding Deformation, Fission Gas Release during Power Transients at High Burnup. LWR Fuel Performance, Williamsburg.

[26] Park, S.Y., Kim, J.H., Lee, M.H. and Jeong, Y.H. (2008) Stress-Corrosion Crack Initiation and Propagation Behavior of Zircaloy-4 Cladding under an Iodine Environment. *Journal of Nuclear Materials*, **372**, 293-303. https://doi.org/10.1016/j.jnucmat.2007.03.258

[27] Le Boulch, D., Fournier, L. and Catherine, C.S. (2004) Pellet-Clad Interaction in Water Reactor Fuels. *Seminar Proceedings*, Aix en Provence, 9-11 March 2004, p. 253. https://www.oecd.org/content/dam/oecd/en/publications/reports/2005/07/pellet-clad-interaction-in-water-reactor-fuels_g1gh5b9b/9789264011588-en.pdf

[28] Rosenbaum, H.S. (1982) GEAP-25163-6. General Electric Company.

[29] Garzarolli, F., von Jan, R. and Stehle, H. (1979) The Main Causes of Fuel Element Failure in Water-Cooled Power Reactors. *Atomic Energy Review*, **7**, 31-128.

[30] Videm, K. and Lunde, L. (1979) In: Papa-Zoglon, T.P., Ed., *Zirconium in the Nuclear Industry*, *Fourth Conference*, *ASTM STP* 681, American Society for Testing and Materials, p. 234.

[31] Mattas, R.F., Yaggee, F.L. and Neimark, L.A. (1982) In: Franklin, D.G., Ed., *Zirconium in the Nuclear Industry*, *Fifth Conference*, *ASTM STP* 754, American Society for Testing and Materials, 158.

[32] Floyd, M. (2001) Proceedings of the Seventh CANDU Fuel Conference, Kingston, 1-20.

[33] Gartner, M. and LaVake, J.C. (1983) Power Ramp Testing and Non-Destructive Post-Irradiation Examinations of High Burnup PWR Fuel Rods. *Proceedings of the IAEA Meeting on Pellet-Cladding Interaction in Water Reactor Fuel*, Seattle, p. 27.

[34] Roberts, J.T.A. (1981) LWR Core Materials. In: Roberts, J.T.A., Ed., *Structural Materials in Nuclear Power Systems*, Springer, 53-136. https://doi.org/10.1007/978-1-4684-7194-6_2

[35] Videm, K. and Lunde, L. (1977) Stress Corrosion Cracking of Zircaloy Fuel Cladding Tubes Under Power Ramps and in Laboratory Tests. American Nuclear Society.

[36] Piro, M.H.A., Sunderland, D., Livingstone, S., Sercombe, J., Revie, W., Quastel, A., Terrani, K. and Judge, C. (2020) 2.09-Pellet-Clad Interaction Behavior in Zirconium Alloy Fuel Cladding. *Comprehensive Nuclear Materials* (*Second Edition*), **2**, 248-306. https://doi.org/10.1016/B978-0-12-803581-8.09799-X

[37] Floyd, M.R., Leach, D.A., Moeller, R.E., Elder, R.R., Chenier, R.J. and O'Brien, D. (1992) Behaviour of Bruce NGS-A Fuel Irradiated to a Burnup of ~500 MWh/kgU. *Proceedings of the Third International Conference on CANDU Fuel*, Pembroke, 1-16.

[38] Lewis, B.J., Thompson, W.T., Kleczek, M.R., Shaheen, K., Juhas, M. and Iglesias, F.C. (2011) Modelling of Iodine-Induced Stress Corrosion Cracking in CANDU Fuel. *Journal of Nuclear Materials*, **408**, 209-223. https://doi.org/10.1016/j.jnucmat.2010.10.063

[39] Hastings, I.J., Tayal, M. and Manzer, A.M. (1990) CANDU Fuel Performance in Load-Following Operation. AECL-9812.

[40] Erbacher, F., Neitzel, H., Rosinger, H., Schmidt, H. and Wiehr, K. (1982) Burst Criterion of Zircaloy Fuel Claddings in a Loss-Of-Coolant Accident. In: Garde, A.M. and Bradley, E.R., Eds., *Zirconium in the Nuclear Industry*, ASTM International, 271-283. https://doi.org/10.1520/stp37058s

[41] Beguin, S. (2005) PCI-Related Constraints on EDF PWRs and Associated Challenges. In: Pellet-Clad Interact. Water React. Fuels, Organisation for Economic Co-Operation and Development, Nuclear Energy Agency, 75, Paris (France); 548 p; Worldcat; Jul 2005; p. 53-62; Seminar: Pellet-Clad Interaction in Water Reactor Fuels; Aix-en-Provence (France); 9-11 Mar 2004, 53-62.

[42] Labrot, G. (1984) Une Ithaque pour immigrés, la gare de Porta Nova à Turin. *Le Monde alpin et rhodanien. Revue régionale d'ethnologie*, **12**, 161-164.

https://doi.org/10.3406/mar.1984.1254

[43] Tasooji, A., Einziger, R. and Miller, A. (1984) Modeling of Zircaloy Stress-Corrosion Cracking: Texture Effects and Dry Storage Spent Fuel Behavior. In: Garde, A.M. and Bradley, E.R., Eds., *Zirconium in the Nuclear Industry*, ASTM International, 595-626. https://doi.org/10.1520/stp34497s

[44] Fish, R.L. and Einziger, R.E. (1981) Rept. HEDL-TME 81-3, Hanford Engrg. Devel. Lab., Richland, WA, 1981.

[45] Schrire, D., Lysell, G., Grigoriev, V. and Josefsson, B. (2000) Proceedings of the IAEA Technical Committee Meeting on Fuel Chemistry and Pellet-Clad Interaction Related to High Burnup Fuel, Vienna, p. 105.

[46] International Atomic Energy Agency (2019) Review of Fuel Failures in Water Cooled Reactors, An Update of IAEA Nuclear Energy Series No. NF-T-2.1. IAEA Vienna.

[47] Ledergerber, G., Valizadeh, S., Wright, J., Limbäck, M., Hallstadius, L., Gavillet, D., *et al.* (2010) TopFuel, 513-524.

[48] Yang, R., Cheng, B., Deshon, J., Edsinger, K. and Ozer, O. (2006) Fuel R&D to Improve Fuel Reliability. *Journal of Nuclear Science and Technology*, **43**, 951-959. https://doi.org/10.3327/jnst.43.951

[49] Birk, S. (2010) Antitrust Measures Support Quality Patient Care. *Internal Medicine News*, **43**, 53. https://doi.org/10.1016/s1097-8690(10)70757-5

[50] Joseph, J., Atabek, R. and Trotabas, M.L. (1982) The CEA-Fragema Ramp Test Programme for the Study of the Effect of Power Cycling on PCI at High Burn-Up. *Proceeding of Specialists MTG on Power Ramping, Cycling Behaviour of Water Reactor Fuels*, Petten, p. 36.

[51] Wood, J.C. (1972) Factors Affecting Stress Corrosion Cracking of Zircaloy in Iodine Vapour. *Journal of Nuclear Materials*, **45**, 105-122. https://doi.org/10.1016/0022-3115(72)90178-x

[52] Piro, M., Sunderland, D., Revie, W., Livingstone, S., Dimayuga, I., Douchant, A., *et al.* (2018) Potential Mitigation Strategies for Preventing Stress Corrosion Cracking Failures in High-Burnup Candu Fuel. *CNL Nuclear Review*, **7**, 127-146. https://doi.org/10.12943/cnr.2016.00011

[53] Miller, A.K., Ocken, H. and Tasooji, A. (1981) Iodine Stress Corrosion Cracking of Zircaloy: Laboratory Data, a Phenomenological Model, and Predictions of In-Reactor Behavior. *Journal of Nuclear Materials*, **99**, 254-268. https://doi.org/10.1016/0022-3115(81)90194-x

[54] Videm, K., Lunde, L., Hollowell, T., Vilpponen, K. and Vitanza, C. (1979) Cracking of Cladding Tubes Caused by Power Ramping and by Laboratory Stress Corrosion Experiments. *Journal of Nuclear Materials*, **87**, 259-267. https://doi.org/10.1016/0022-3115(79)90562-2

[55] Sejnoha, R. and Wood, J. (1979) Iodine-induced Stress Corrosion Cracking of Fixed Deflection Stressed Slotted Rings of Zircaloy Fuel Cladding. In: Garde, A.M. and Bradley, E.R., Eds., *Zirconium in the Nuclear Industry*, ASTM International, 261-284. https://doi.org/10.1520/stp36685s

[56] Farahani, M., Chan, P.K., Corcoran, E.C., Hameed, R. and Torkelson, T. (2019) Strategies in Mitigating Stress Corrosion Cracking of Zircaloy-4 Fuel Sheathing: A Case for Polysiloxane Coating. 14*th International Conference on CANDU Fuel*, Mississauga, 21-24 July 2019, p. 10.

[57] Farahani, M., Ferrier, G.A., Chan, P.K. and Corcoran, E.C. (2013) Beyond CANLUB: An Improved Alternative Coating Development. 12*th International Conference on*

CANDU Fuel, Kingston, 15-18 September 2013, 1-14.

[58] Hoppe, N. and Thomas, G.R. (1978) EPRI.

[59] Heckman, H. and Strasser, A. (1978) American Nuclear Society Topical Meeting on Water Reactor Fuel Performance, 189-196.

[60] Cox, B. (1990) Environmentally-induced Cracking of Zirconium Alloys—A Review. *Journal of Nuclear Materials*, **170**, 1-23. https://doi.org/10.1016/0022-3115(90)90321-d

[61] Quastel, A.D., Corcoran, E.C. and Lewis, B.J. (2013) The Effect of Oxidized UO2 on Iodine Induced Stress Corrosion Cracking of Fuel Sheathing. 12*th International Conference on CANDU Fuel*, Kingston, 15-18 September 2013, 1-14.

[62] Blake, A. (1990) Practical Stress Analysis in Engineering Design. 2nd Edition, Marcel Dikker, Inc., 292-294.

[63] Rosinger, H.E. and Northwood, D.O. (1979) The Elastic Properties of Zirconium Alloy Fuel Cladding and Pressure Tubing Materials. *Journal of Nuclear Materials*, **79**, 170-179. https://doi.org/10.1016/0022-3115(79)90444-6

[64] Oding, I.A., Ivanova, V.S., Burdukskii, V.V. and Geminov, V.N. (1965) Creep and Stress Relaxation in Metals. Oliver and Boyd, 270-271.

[65] Ferrier, G.A., Metzler, J., Farahani, M., Chan, P.K. and Corcoran, E.C. (2014) Dynamic Thermo-Chemo-Mechanical Strain of Zircaloy-4 Slotted Rings for Evaluating Strategies That Mitigate Stress Corrosion Cracking. *The* 19*th Pacific Basin Nuclear Conference*, Vancouver, 24-28 August 2014. https://www.osti.gov/etdeweb/biblio/22670344

[66] Waheed, A., Palleck, S., Chakraborthy, K. and Roth, M. (2008) Fatigue Tests on CANDU Fuel, Zircaloy Tubes for AECL Loading Following Program—Romania. 10*th CNS International Conference on CANDU Fuel*, Ottawa, 5-8 October 2008. https://www.osti.gov/etdeweb/biblio/21296872

[67] Lemoine, P., Darchis, L., Pelchat, J., Mardon, J.P. and Grosgeorge, M. (1988) Sustained Fatigue of Zircaloy-4 Claddings—Non-Irradiated Material. *IAEA Technical Committee Meeting on Power Ramping, Cycling, and Load Following Behaviour of Water Reactor Fuel*, Lyon, 45-54.

[68] Jezequel, T., Auzoux, Q., Le Boulch, D., Bono, M., Andrieu, E., Blanc, C., *et al.* (2018) Stress Corrosion Crack Initiation of Zircaloy-4 Cladding Tubes in an Iodine Vapor Environment during Creep, Relaxation, and Constant Strain Rate Tests. *Journal of Nuclear Materials*, **499**, 641-651. https://doi.org/10.1016/j.jnucmat.2017.07.014

[69] Haddad, R. and Dorado, A. (1994) Grain-by-Grain Study of the Mechanisms of Crack Propagation during Iodine Stress Corrosion Cracking of Zircaloy-4. In: Garde, A.M. and Bradley, E.R., Eds., *Zirconium in the Nuclear Industry*: *Tenth International Symposium*, ASTM International, 559-575. https://doi.org/10.1520/stp15209s

[70] Jacques, P., Lefebvre, F. and Lemaignan, C. (1999) Deformation-Corrosion Interactions for Zr Alloys during I-SCC Crack Initiation. *Journal of Nuclear Materials*, **264**, 239-248. https://doi.org/10.1016/s0022-3115(98)00501-7

[71] Farina, S.B., Duffo, G.S. and Galvele, J.R. (2002) Corrosion'2002, 57th Annual Conf. & Exposition, Denver, 7-12 April 2002, Paper No. 02436.

[72] Jalilibal, Z., Amiri, A., Castagliola, P. and Khoo, M.B.C. (2021) Monitoring the Coefficient of Variation: A Literature Review. *Computers & Industrial Engineering*, **161**, Article ID: 107600. https://doi.org/10.1016/j.cie.2021.107600

[73] Ferrier, G.A., Farahani, M., Metzler, J., Chan, P.K. and Corcoran, E.C. (2016) J. Nucl. Eng. Radiat. Sci., 2, 21004, 2016.

[74] Totten, G. (2005) Handbook on Residual Stress, Vol. 1. SEM.

[75] Cox, B. and Haddad, R. (1987) Recent Studies of Crack Initiation during Stress Corrosion Cracking of Zirconium Alloys. In: Garde, A.M. and Bradley, E.R., Eds., *Zirconium in the Nuclear Industry*, ASTM International, 717-733. https://doi.org/10.1520/stp28155s

[76] Cox, B. (1977) Transient Species Participating in the SCC of Zirconium Alloys. *Corrosion*, **33**, 79-84. https://doi.org/10.5006/0010-9312-33.3.79